Design of New Hybrid-Ring Directional Coupler Using $\lambda/8$ or $\lambda/6$ Sections

Dong Il Kim, Gyu-Sik Yang, Se-Mo Chung

1/8 또는 1/6파장 선로를 이용한 새로운 형식의 하이브리드 링 방향성 결합기의 설계

김동일*·양규식*·정세모**

Abstract

A design method of the new 1.25λ-ring and $7\lambda/6$-ring 3 dB directional coupler using fundametal $\lambda/8$-or $\lambda/6$-sections is proposed and their frequency characteristics are analyzed.

Furthermore, the experimental verification has been achieved in microstrip network, and, hence, the validity of the design method of a microwave component with the basic $\lambda/8$-or $\lambda/6$-sections proposed in this paper is confirmed.

1. Introduction

The hybrid-ring directional coupler is one of the earliest and fundamental junctions in microwave and millimeterwave frequency band[1-6], which has one-axis symmetry. The important common properties possessed by all directional couplers are : 1) the output arms are isolated from each other, and 2) the input arms are macthed looking into any arm when the other arms are terminated by matched loads. Since the conventional simple Y-junction power dividers do not possess these properties, directional couplers are preferable for certain applications, such as antenna array feed systems where the need for minimizing mutual coupling puts a premium on

* 한국해양대학 전자통신공학과
** 한국해양대학 항해학과

isolation between the output arms of the power dividers[2].

The two-dimensional structure of stripline facilitates construction of the feeding network and antenna elements, such as dipoles on a single printed circuit board. At high frequencies, some applications make hybrid-ring couplers preferable to branch-line and parallel-line couplers; the former has an inherent 90° phase difference between the output ports. For an antenna array that is fed by an equiphase, symmetrical, corporate network, the hybrid-ring directional coupler has a definite advantage over the parallel-line and branch-line couplers because no phase compensating element is necessary. The hybrid-ring coupler also has a broader bandwidth than the branch-line coupler[2),4)].

A hybrid-ring directional coupler is well known as a rat race ring which is used for a 3-dB directional coupler with the normalized admittance of $1/\sqrt{2}$ on the whole circumfaerence on the ring[2]. In 1961 C. Y. Pon proposed the design method of a hybrid-ring coupler, the power-split ratio by which is propotional to the square of the admittance ratio of the two variable admittances in the ring[2]. In 1982, D. I. Kim and Y. Naito developed a broad-band design method of improved hybrid-ring 3dB directional couplers by CAD, where the concept of a hypothetical port was adapted[5]. In 1986, A. K. Agrawal and G. F. Mikucki have designed a hygrid-ring directional coupler with arbitrary power divisions by adapting C. Y. Pon's method to Kim and Naito's concept of a hypothetic port[4]. However, all of branch-line couplers, parallel-line couplers, and hybrid-ring couplers including rat race ring, consist of common fundametal $\lambda/4$-sections. In addition, most microwave components also use fundamental $\lambda/4$-lines.

In this paper, however, we propose a design method of the 1.25λ-ring and the $7\lambda/6$-ring 3 dB directional couplers not by using fundamental $\lambda/4$-secitons but by using $\lambda/8$-and $\lambda/6$-sections, respectively. In addition, the frequency characteristics of the couplings, the isolations, return losses, and the phase differences between the output ports are also calculated.

II. Analysis and Design of $\lambda/8$-and $\lambda/6$-ring 3dB Directional Couplers

The conventional hybrid-ring directional coupler has the configuration as shown in Fig.1[2].

To increase the degree of freedom of design, while maintaining symmerty, the characteristic admittance Y_1 of the $3\lambda/4$-section across the symmetrical axis AA' can be replaced by Y_3, and the lengths $\lambda/4$ and $3\lambda/4$ of two sections across the symmetrical axis AA' by $\lambda/8$ and $5\lambda/8$, respectively. Then, the circumference of the ring of the directional coupler becomes 1.25λ as shown in Fig.2, which is referred to as the 1.25λ-ring directional coupler here.

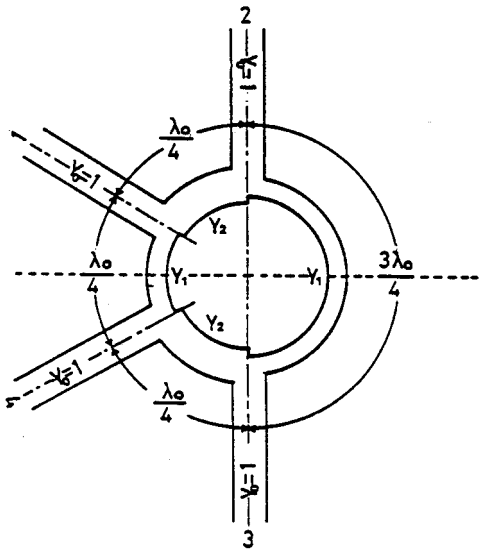

Fig 1. Conventional Hybrid-ring Directional Coupler

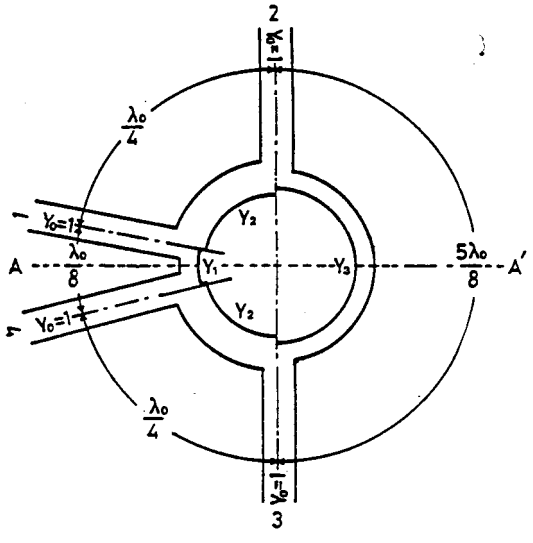

Fig 2. Configuration of an 1.25 wavelength hybrid-ring

As the same as the above, the lengths $\lambda/4$, $\lambda/4$ and $3\lambda/4$ of the sections Y_1, Y_2 and $4\lambda/6$ as shown in Fig.3, which is referred to as the $7\lambda/6$-ring directional coupler since the whole cireumference on the ring is $7\lambda/6$.

II-1. Analysis of Frequency Resopnse Characteristics

To analyze the frequency response characteristics of the proposed 1.25λ-ring and the $7\lambda/6$-ring directional couplers, we represent the equivalent circuits for the couplers as shown in Fig.4.

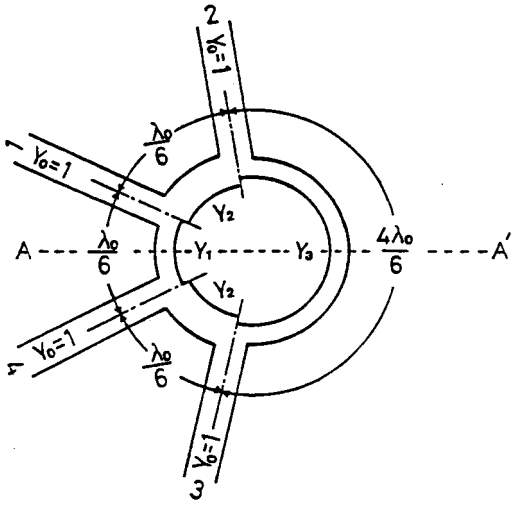

Fig 3. Configuration of a 7/6 wavelength hybrid-ring

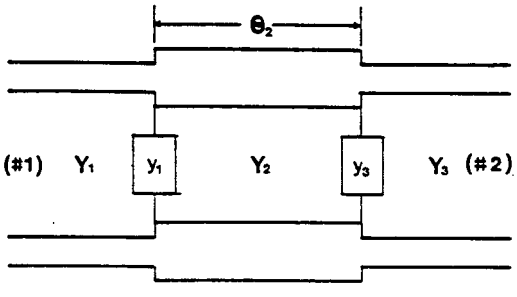

Fig 4. Equivalent Circuti for Even of Odd Mode Excitaion

Then, the values of y_1 and y_3 for the even and the odd mode excitations can be represented by y_1^e and y_3^e, and y_1^o and y_3^o as follows:

① For the even mode excitation of ports 1 and 4,

$$y_1^e = jY_1\tan(\theta_1/2)$$
$$y_3^e = jY_3\tan(\theta_3/2) \tag{1}$$

② For the odd mode excitation of ports 1 and 4,

$$y_1^o = jY_1\cot(\theta_1/2)$$
$$y_3^o = -jY_3\cot(\theta_3/2) \tag{2}$$

where, $\theta_1=\theta_0/2$, $\theta_2=\theta_0$, and $\theta_3=5\theta_0/2$ for 1.25λ-ring directional coupler and $\theta_1=2\theta_0/3$, $\theta_2=2\theta_0/3$, and $\theta_3=8\theta_0/3$ for the $7\lambda/6$-ring direrctional coupler, respectively. The follwing relations are also standing for.

$$\theta_0=\pi\lambda_0/2\lambda_g=\pi f/2f_o \tag{3}$$

where, λ_0 is the wavelength at the designed center frequency, λ_g is the guided wavelength, f_0 is the design center frequency, and f is the frequency, respectively.

Since the ABCD-matrix[F] for the equivalent circuti shown in Fig.4 is given by

$$[F]=\begin{pmatrix}1 & 0\\ y_1 & 1\end{pmatrix}\begin{pmatrix}\cos\theta_2 & j\sin\theta_2/Y_2\\ jY_2\sin\theta_2 & \cos\theta_2\end{pmatrix}\begin{pmatrix}1 & 0\\ y_3 & 1\end{pmatrix} \tag{4}$$

the scattering elements can be obtained by found as following steps. Substituting for the calculated values of y_1^e and y_3^e, and y_1^o and y_3^o from eqs.(1) and (2) into eq.(4), respectively, the intrinsic reflection coefficients of Γ_e and Γ_o, and the intrinsic transmission coefficients of T_e and T_o can be calculated by eq.(5).

$$\Gamma_e=\frac{A+B-C-D}{A+B+C+D}\Big|_e$$
$$\Gamma_o=\frac{A+B-C-D}{A+B+C+D}\Big|_o$$
$$T_e=\frac{2}{A+B+C+D}\Big|_e \tag{5}$$
$$T_o=\frac{2}{A+B+C+D}\Big|_o$$

Thus the scattering parameters, i.e., the frequency characteristics, can be easily obtained using eqs. (5), (9), and (11). The elements A, B, C, and D of $[F]^e$ and $[F]^o$ in eq.(5) are as follows when the input port is #1 or #4.

$$[F]^e=\begin{pmatrix} \cos\theta_2+(Y_3/Y_2)\tan(\theta_3/2)\sin\theta_2 & j(1/Y_2)\sin\theta_2 \\ j[\{Y_1\tan(\theta_1/2)+Y_3\tan(\theta_3/2)\}\cos\theta_2 & \cos\theta_2-(Y_1/Y_2)\tan(\theta_1/2)\sin\theta_2 \\ +\{Y_2-(Y_1Y_3/Y_2)\tan(\theta_1/2)\tan(\theta_2/2)\}\sin\theta_2] & \end{pmatrix}$$

$$[F]^o=\begin{pmatrix} \cos\theta_2+(Y_3/Y_2)\cot(\theta_3/2) & j(1/Y_2)\sin\theta_2 \\ -j[\{Y_1\cot(\theta_1/2)+Y_3\cot(\theta_3/2)\}\cos\theta_2 & \cos\theta_2+(Y_1/Y_2)\cot(\theta_1/2)\sin\theta_2 \\ +\{(Y_1Y_3/Y_2)\cot(\theta_3/2)-Y_2\}\sin\theta_2] & \end{pmatrix} \quad (6)$$

and when the input port is #2 or #3,

$$[F]^o=\begin{pmatrix} \cos\theta_2-(Y_1/Y_2)\tan(\theta_2/2)\sin\theta_2 & j(1/Y_2)\sin\theta_2 \\ j[\{Y_1\tan(\theta_1/2)+Y_3\tan(\theta_3/2)\}\cos\theta_2 & \cos\theta_2-(Y_3/Y_2)\tan(\theta_3/2)\sin\theta_2 \\ +\{Y_2-(Y_1Y_3/Y_2)\tan(\theta_3/2)\}\sin\theta_2] & \end{pmatrix}$$

$$[F]^o=\begin{pmatrix} \cos\theta_2+(Y_1/Y_2)\cot(\theta_1/2) & j(1/Y_2)\sin\theta_2 \\ -j[\{Y_1\cot(\theta_1/2)+Y_3\cot(\theta_3/2)\}\cos\theta_2 & \cos\theta_2+(Y_3/Y_2)\cot(\theta_3/2)\text{son}\theta_2 \\ +\{(Y_1Y_3/Y_2)\cot(\theta_3/2)-Y_2\}\sin\theta_2] & \end{pmatrix} \quad (7)$$

II. Design of 1.25λ-and 7λ/6-ring 3dB Directional Couplers

In general< the scattering matrix [S]representing the input-output relation for a reciprocal junction with one-axis symmetry, as shown in Figs. 1, 2, and 3, is represented by eq.(8).

$$[S]=\begin{pmatrix} S_{11} & S_{12} & S_{13} & S_{14} \\ S_{21} & S_{22} & S_{23} & S_{24} \\ S_{31} & S_{32} & S_{33} & S_{34} \\ S_{41} & S_{42} & S_{43} & S_{44} \end{pmatrix}=\begin{pmatrix} S_{11} & S_{12} & S_{13} & S_{14} \\ S_{12} & S_{22} & S_{23} & S_{13} \\ S_{13} & S_{23} & S_{22} & S_{12} \\ S_{14} & S_{13} & S_{12} & S_{11} \end{pmatrix} \quad (8)$$

Using these scattering parameters, 1.25λ-ring and the 7λ/6-ring directional couplers can be

designed.

[A] 1.25-ring directional coupler

Substituting eqs. (1) and (2) into eqs. (6) and (7), respectively, and putting $Y_1=Y_3$, $\theta_0=\pi/2$, $\theta_1=\pi/4$, $\theta_2=\pi/2$ and $\theta_3=5\pi/4$, the scattering parameters for the 1.25λ-ring are calculated as follows; When the input port is #1 or #4 in the 1.25λ-ring directional coupler, the intrinsic reflection coefficients Γ_e and Γ_o, and the intrinsic transmission coefficients T_e and T_o are given by eq.(9).

$$\begin{aligned}\Gamma_e&=\frac{2\sqrt{2}Y_1+j(1-Y_2^2-Y_1^2)}{2Y_1+j(1+Y_2^2+Y_1^2)}\\ \Gamma_o&=\frac{-2\sqrt{2}Y_1+j(1-Y_2^2-Y_1^2)}{2Y_1+j(1+Y_2^2+Y_1^2)}\\ T_e&=\frac{2Y_2}{2Y_1+j(1+Y_2^2+Y_1^2)}\\ T_o&=\frac{2Y_2}{2Y_1+j(1+Y_2^2+Y_1^2)}\end{aligned}\tag{9}$$

Similarly, when the input port is #2 or #3 in the 1.25λ-ring, Γ_e and Γ_o, and T_e and T_o are given by eq.(10)

$$\begin{aligned}\Gamma_e&=\frac{-2\sqrt{2}Y_1+j(1-Y_2^2-Y_1^2)}{2Y_1+j(1+Y_2^2+Y_1^2)}\\ \Gamma_o&=\frac{2\sqrt{2}Y_2+j(1-Y_1^2-Y_2^2)}{2Y_1+j(1+Y_1^2+Y_2^2)}\\ T_e&=\frac{2Y_2}{2Y_1+j(1+Y_1^2+Y_2^2)}\\ T_o&=\frac{2Y_2}{2Y_1+j(1+Y_1^2+Y_2^2)}\end{aligned}\tag{10}$$

thus, the scattering parameters are found by eq.(11).

$$\begin{aligned}S_{11}&=(1/2)(\Gamma_e+\Gamma_o)=\frac{j(1-Y_1^2-Y_2^2)}{2Y_1+j(1+Y_1^2+Y_2^2)}\\ S_{41}&=(1/2)(\Gamma_e-\Gamma_o)=\frac{2\sqrt{2}Y_1}{2Y_1+j(1+Y_1^2+Y_2^2)}\\ S_{21}&=(1/2)(T_e+T_o)=\frac{2Y_2}{2Y_1+j(1+Y_1^2+Y_2^2)}\\ S_{22}&=(1/2)(\Gamma_e+\Gamma_o)=S_{11}\\ S_{32}&=(1/2)(\Gamma_e-\Gamma_o)=-S_{41}\\ S_{12}&=S_{21}\\ S_{42}&=S_{31}=0\end{aligned}\tag{11}$$

From eq. (11) we can see that two output arms are isolated from each other since $S_{31}=S_{42}=0$. The condition that the input arm ve perfectly matched requires that S_{11} and S_{22} in eq.(11) be zero, from which we get

$$Y_1^2+Y_2^2=1, \tag{12}$$

and the condition for 3dB output power division requires that $|S_{21}|=|S_{41}|$ and $|S_{12}|=|S_{32}|$ in eq. (11), from which we get

$$Y_2=2Y_1. \tag{13}$$

Thus, the 1.25λ-ring 3dB directional coupler can be designed by taking $Y_1=1/\sqrt{3}$ and $Y_2=\sqrt{2/3}$ which can be seen from eqs. (12) and (13), and the output voltage ratio(couplings) between the output arms can be adjusted by varying Y_1 and Y_2.

[B] $7\lambda/6$-ring Directional Coupler

Substituting, in the same manner as the above, eqs.(1) and (2) into eqs.(6) and (7), respectively, and $Y_1=Y_3$, $\theta_0=\pi/2$, $\theta_1=\theta_2=2\theta_0/3$, and $\theta_3=8\theta_0/3$, the scattering parameters for the $7\lambda/6$-ring are calculated as follows;

When the input port is #1 or #4, the scattering parameters are after finding the intrinsic reflection coefficients Γ_e and Γ_0 and the transmission coefficients T_e and T_0 as the same manner as eqs.(9) and (10).

$$\begin{aligned}
S_{11}&=(1/2)\frac{j\{\sqrt{3}+(2\sqrt{3}/3)\,Y_1Y_2-\sqrt{3}Y_2^2-(\sqrt{3}Y_1^2\}}{Y_1+Y_2+j\{(\sqrt{3}/2)-(\sqrt{3}/3)\,Y_1Y_2+(\sqrt{3}/2)\,Y_2^2+(\sqrt{3}/2)\,Y_1^2\}}\\
S_{41}&=(1/2)\frac{4Y_1}{Y_1+Y_2+j\{(\sqrt{3}/2)-(\sqrt{3}/3)\,Y_1Y_2+(\sqrt{3}/2)\,Y_2^2+(\sqrt{3}/2)\,Y_1^2\}}\\
S_{21}&=(1/2)\frac{4Y_2}{Y_1+Y_2+j\{\sqrt{3}/2)-(\sqrt{3}/3)\,Y_1\phi_2+(\sqrt{3}/2)\,Y_2^2+(\sqrt{3}/2)\,Y_1^2\}}\\
S_{42}&=0
\end{aligned} \tag{14}$$

When the input port is #2 or #3, on the other hand, the scattering parameters are given by eq. (15).

$$\begin{aligned}
S_{22}&=(1/2)\frac{j\{\sqrt{3}+(2\sqrt{3}/3)\,Y_1Y_2-\sqrt{3}Y_2^2-(\sqrt{3}Y_1^2)\}}{Y_1+Y_2+j\{(\sqrt{3}/2)-(\sqrt{3}/3)\,Y_1Y_2+(\sqrt{3}/2)\,Y_2^2+(\sqrt{3}/2)\,Y_1^2\}}=S_{11}\\
S_{32}&=(1/2)\frac{-4Y_1}{Y_1+Y_2+j\{(\sqrt{3}/2)-(\sqrt{3}/3)\,Y_1Y_2+(\sqrt{3}/2)\,Y_2^2+(\sqrt{3}/2)\,Y_1^2\}}=-S_{41}
\end{aligned} \tag{15}$$

$$S_{12}=(1/2)\frac{4Y_2}{Y_1+Y_2+j\{(3/2)-(3/3)Y_1Y_2+(3/2)Y_2^2+(3/2)Y_1^2\}}=S_{21}$$

$$S_{42}=0=S_{31}$$

From the eqs.(14) and (15) we can see that two output ports are isolated each other since $S_{31}=S_{42}=0$ at $f=f_o$. The condition for 3dB output power division requires that $|S_{21}|=|S_{41}|$ and $|S_{12}|=|S_{32}|$ In eqs (14) and (15), respectively, form whcih we get

$$Y_1=Y_2=Y, \tag{16}$$

and the condition that the input arm is perfectly mached requires that S_{11} and S_{22} in eqs.(14) and (15) be zero, from which we got

$$Y=\sqrt{3/4} \tag{17}$$

Thus, it has been shown that the $7\lambda/6$-ring 3dB directional coupler can be designed by taking the normalized characteristic admttance Y as 3/4 on the whole circumferece.

III. Theoretical Frequency Characteristics

Fig.5(a) shows the theoretical frequency characteristics of coupling, reflection, and isolation for the 1.25λ-ring 3dB directional coupler designed in II, while Fig.5(b) shows the phase differences

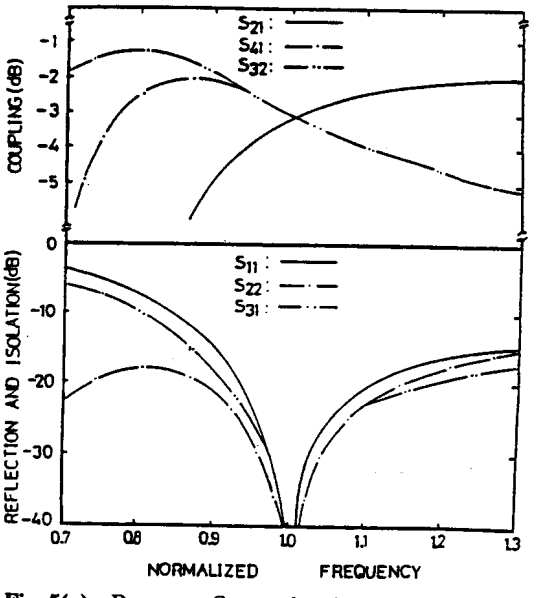

Fig 5(a). Response Curves for the 1.25 wavelength hybrid-ring
(coupling, Isolation, and Reflection)

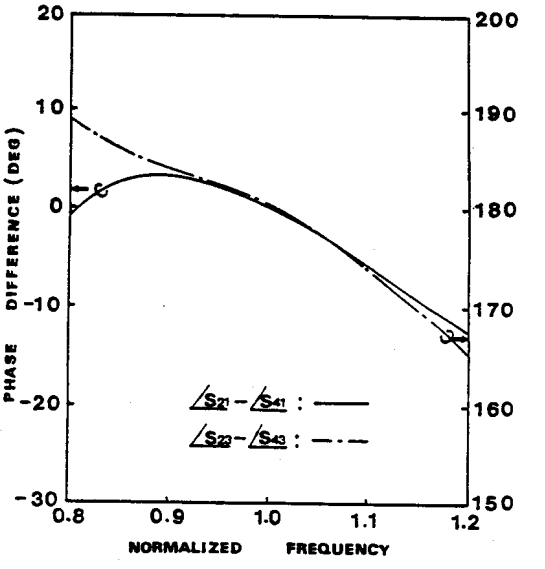

Fig 5(b). Phase differences between outputs of the 1.25 wavelength hybrid-ring

Table 1. Designed 7λ/6-ring Hybrid Coupler Table

Section	Y_1	Y_2	Y_3
Normalized Characteristic Admittance	3/4	3/4	3/4
length of each section	λ/6	λ/6	2λ/3

2. Designe 1.25λ-ring Hybrid Coupler

Section	Y_1	Y_2	Y_3
Normalized Characteristic Admittance	1/ 3	2/3	1/ 3
length of each section	λ/6	λ/6	2λ/3

between outputs for the coupler. The characteristic admittance and the length of each section are represented in Table 1.

Fig.6(a) shows the the oretical frequency characteristics of coupling, reflection, and isolation for the 7λ/6-ring 3dB directional coupler designed in II, while Fig.6(b) shows the phase differences between outputs for the coupler. The characteristic admittance and the length of each section are represented in Table 2.

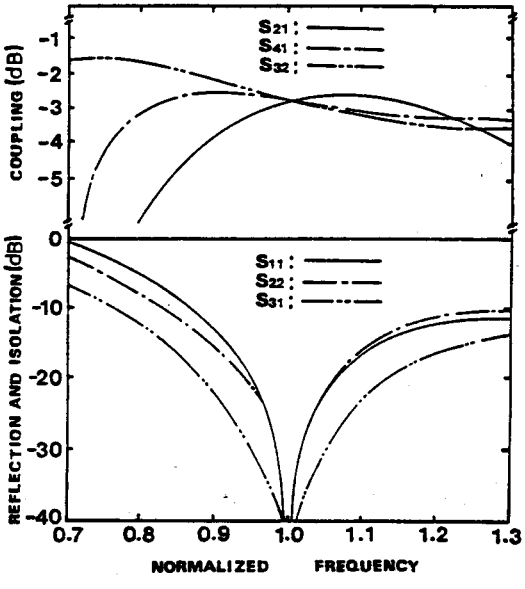

Fig 6(a). Response Curves for the 7/6 wavelength hybrid-ring (coupling, Isolation, and Reflection)

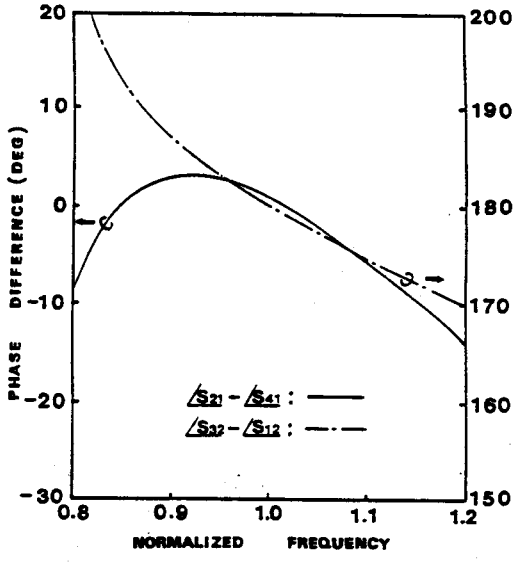

Fig 6(b). Phase differences between outputs of the 7/6 wavelength hybrid-ring

IV. Experimetal Results

To confirm the validity of the proposed design method of the new 3dB hybrid-ring directional couplers, we have fabricated the circuits as shown in Table 3 and Table 4 on microstrip line and tested their frequency characteristics. The effective dielectric constant, the wavelength, the line-

width, and the line impedance in the microstrip have been calculatd by [8] and [9]. The calculated values for constructing the proposed new 3dB hybrid-rings at the center frequency of 9.4GHz are tabulated in Table 3 and Table 4.

Table 3. Values for Fabrication of the Designed 3-dB Hybrid-ring directional Coupler Used in Experiments

Sections	Normalized Admittance	ε_{eff}	λ_g(mm)	Line width(mm)
$Y_1=Y_3$	0.577	2.026	22.422	0.625
Y_2	0.816	2.103	22.008	1.202

* the relative dielectric constant $\varepsilon_r=2.60$
the thickness of substrate h=0.6mm
the design center frequency $f_0=9.4$GHz
the loss tangent $\tan\delta=0.0022$

Table 4. Values for Fabrication of the Designed 3-dB Hybrid-ring directional Coupler Used in Experiments

Sections	Normalized Admittance	ε_{eff}	λ_g(mm)	Line width(mm)
$Y_1=Y_2=Y_3$	0.866	2.116	21.94	1.327

* The relative dielectric constant, etc are the same as those in Table 3.

Figs. 7 and 8 show the circutis fabricated and used for experiments, one of which is the 1.25λ -ring and the other is the 7λ/6-ring directional coupler. Because of the variation in effective dielectric constant in microstrip, the lengths of the sections on the ring circumference should be different form one another. However, in the experiments we constructed the networks conveniently and easily by using the mean value of the wavelengths on the circumference, i.e., neglecting the differences of the wavelengths due to the differences of the line impedances.

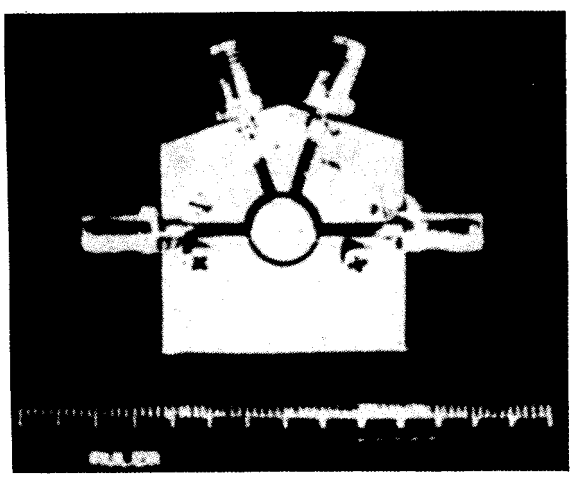

Fig 7. Photograph of the Fabricated 1.25λ-ring Directional Coupler

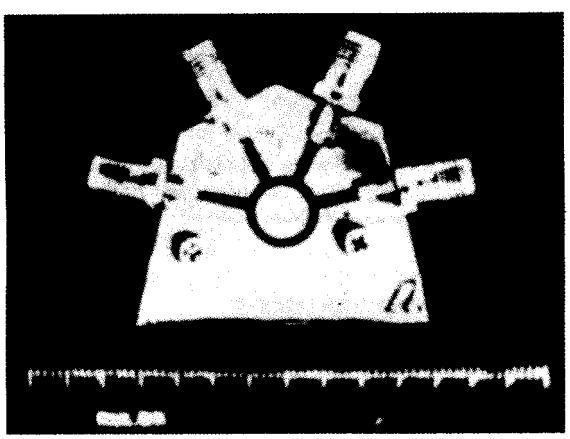

Fig 8. Photograph of the Fabricated 7λ/6-ring Directional Coupler

Fig.9 and 10 show the measured frequency characteristics obtained from the experiments for the proposed new 3dB directional couplers with 1.25λ-ring and 7λ/6-ring circumferences constructed approximately and easily by the previous manner, while the theoretical responses are shown in Figs.5(a) and 6(a), respectively. The frequency characteristics agreed resonably well with the designed ones in spite of neglecting the wavelength differences at the ring sections.

On the other hand, the levels of equal splits were about 3.3dB due to loss this is much improved compared with [5] in spite of the high frequency band. Therefore, the insertion losses are decrease short length of the ring circumferences by using λ/8 or λ/6 lines.

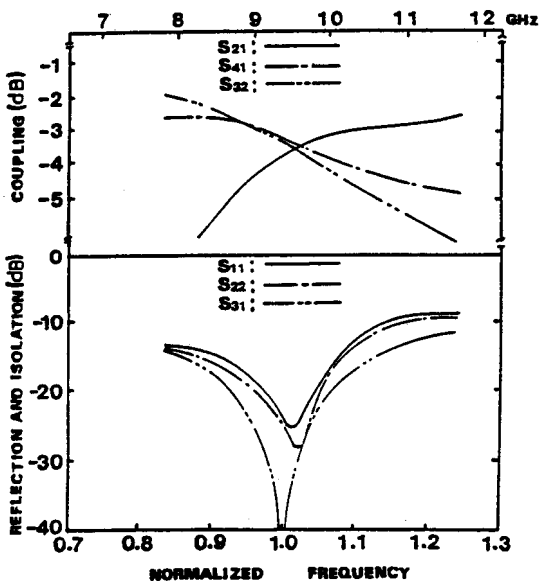

Fig 9. Measured Response Curves ofr the 1.25λ-ring Directional Coupler

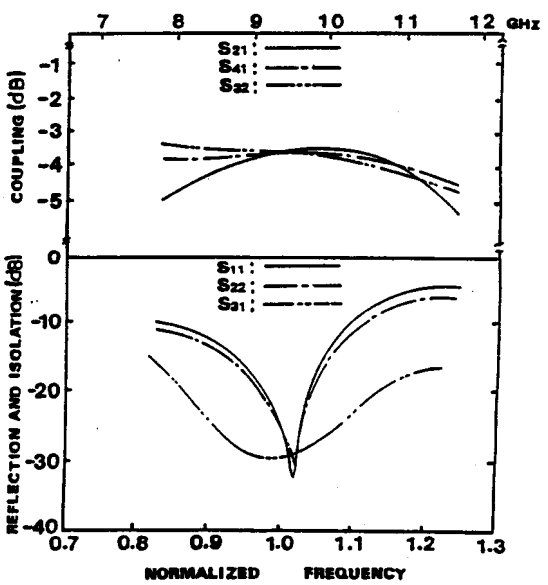

Fig 10. Measured Response Curves ofr the 7λ/6-ring Directional Coupler

V. Conclusion

A new design theory of 3dB hybrid-ring directional couples using λ/8 or λ/6 line was proposed. Moreover, the new 1.25λ-ring and the new 7λ/6-ring directional couplers have been designed and analyzed.

Furthermore, the experiments for the both cases were carried out, the results of which is agreed well with is the theoretical ones, and hence, the validity of the proposed design method was confirmed.

Acknowledgment

The authors would like to express their thanks to the members of the Korea Science & Engineering Foundation, by which this work was sponsored.

References

1) W.V. Tyminski and A.Z. Hylas, "A Wide-Band Hybrid Ring for UHF", Proc. IRE, Vol. 41, pp. 81-87, Jan . 1953.
2) C.Y. Pon "Hybrid-Ring Directional Coupler for Arbitrary Power Division", IRE Trans. on MTT Vol. 9, pp. 529-535, Nov. 1961.
3) M. Arditi, "Characteristics and Applications of Microstrip for Microwave Wiring", IRE Trans. on MTT, Vol. 3, No. 2, pp. 31-56, Mar. 1955.
4) K. Agrawal and G.F. Mikucki, "A Printed-Ciruit Hybrid-Ring Directional Coupler for Arbitrary Power Divisions", IEEE Trans. on MTT, Vol. 34, No. 12, pp. 1401-1407, Dec. 1986.
5) Dong Il Kim and Y. Natio, "Broad-Band Design of the Improved Hybrid-Ring 3dB Directional Coupler", IEEE Trans. on MTT, Vol. 30, No. 11, pp. 2040-2046, Nov. 1982.
6) W.A. Tyrrell, "Hybrid Circuits for Microwaves", Proc. of the IRE, Vol. 35, No. 11, pp. 1294-1306, Nov, 1947.
7) J. Reed and G.J. Wheeler, "A Method of Analysis of Symmetrical Four-Port Network", IRE Trans. MTT, Vol. 4, pp. 246-252, Oct. 1956.
8) M.V. Schneider, "Microstrip line for Microwave Integrated Circutits", Bell Syst. Tech. J., pp. 1421-1445, May-June 1969.
9) Vincent F. Fusco, Microwave Circuit Analysis and Computer Aided Design, Prentice Hall, 1987.